International Journal of Applied Power Engineering (IJAPE)
Vol. 11, No. 1, March 2022, pp. 33~51
ISSN: 2252-8792, DOI: 10.11591/ijape.v11.i1.pp33-51

Comprehensive analysis and design of furnace oil-based power station using ETAP

Raheel Muzzammel, Rabia Arshad
Department of Electrical Engineering, Faculty of Engineering Technology, University of Lahore, Lahore, Pakistan

Article Info

Article history:

Received Aug 10, 2021
Revised Jan 11, 2022
Accepted Jan 22, 2022

Keywords:

Economic dispatch
ETAP Software
Load flow analysis
Motor starting analysis
Power plant
Short circuit analysis
Transient anlaysis

ABSTRACT

High standards of living are linked with the availability of energy. Therefore, there is always a requirement to modify existing power generating systems or to add new systems to fulfill the increasing demands of energy. It is becoming a core issue in the South Asian region so that at least current standards of living could be maintained by controlling growing energy rates and shortening the availability of conventional sources. Furnace oil is a residue obtained in the process of distillation of crude oil in the petroleum industry. This furnace oil is applicable for power generation plants allied with the petroleum industry so that residue of oil refineries could be utilized. In this research, a furnace oil-based power plant is designed in electrical transient and analysis program (ETAP) software. Moreover, steady-state and transient analysis of the proposed design of the power plant are conducted to increase practical viability of model. Load flow is analyzed to depict the performance of the power plant model under load conditions. This model is further tested under the motor starting event to analyze the current drawn by the motor. This event helps to determine the permissible values of protective equipment installed in power plants. In the last, economic dispatch analysis is conducted to find the relative minima of generation cost of furnace oil-based power plant with respect to coal and hydel generation

Corresponding Author:

Raheel Muzzammel
Department of Electrical Engineering, Faculty of Engineering Technology, University of Lahore
1 KM, Off Defense Road, Lahore 54000, Punjab, Pakistan
Email: raheelmuzzammel@gmail.com, raheel.muzzammel@ee.uol.edu.pk

1. INTRODUCTION

With the increasing electricity demand, there is always a need to go for alteration of existing power generating systems and to add new generating units. These additions and modifications must be technically adequate and economically feasible in times of growing electricity rates and load densities. Developing countries like Pakistan have been facing energy shortages for the last decade. Therefore, it is the need time in developing countries to add new generating units so that sustainability in investment and economy could be obtained [1], [2].

Furnace oil is a residue obtained as a result of the distillation process of oil refineries. This furnace oil is useful for the generation of electricity. Therefore, oil refineries are highly motivated in the Middle East where oil reserves are very massive, to install power generating units so that residue of oil refineries could be utilized beneficially [3].

Design of power plant is linked with few analyses without which power plants could not be termed as functional. Among them, the load flow analysis is the key to the acquire steady state of the system [4]–[16]. It is not possible to conduct load flow analysis by handy calculations when the power system is big. In the literature, different linear and nonlinear techniques are available to depict the performance of power systems under steady-state conditions. These techniques are evaluated in terms of their complexity and computational time. Electrical transient and analysis program (ETAP) software is equipped with the Gauss-Seidel iterative technique and Newton Raphson technique. In large and complex power systems, Newton Raphson is found more effective because of less computational time and fewer iterations for convergence. Therefore, its convergence rate is faster. Adaptive Newton Raphson is also available but because of zeros in off-diagonal entries, its convergence rate is rapid but its result loses effectivity because of lost or little information [4]–[7].

The efficiency and reliability of a power system can only be determined by testing its performance under abnormal or faulty conditions. The short circuit is a condition in which current increases rapidly with a sudden drop of voltage at the faulty point. The power system is required to be operated under this condition. Equipment involved in the power system must have the ability to sustain its operation under such abnormalities. Protective equipment installed must have the ability to respond to such abnormalities as desired. In addition to this, this analysis also helps to determine the operating limits of the system, sizing of equipment, and rating of power system components [11], [17]–[19].

The phenomenon of motor starting is also an important event in the power system because of starting characteristics of the motor. 85 percent of motors installed in power systems are induction motors. It draws six to eight times larger current as compared to its rated current at the time of starting. An increase in current makes this event very similar to the event of a fault. Therefore, it needs to be discriminated among these events [20]–[23].

There are events in the power system which increase current for a very short interval of time. These events are mostly termed transients. These events decay down on their own or it needs just a restart of the system at a low scale. Therefore, steady-state events must be differentiated from transient events as steady-state events are required to be rectified [24]–[39].

Cost of generation is an important pillar of any power generating unit. New installations must be reasonably economical so that consumers and supply company's relationship could be derived in an optimum way. Economic dispatch is a way to determine the optimal generating cost from a particular plant while taken into consideration other power generating units. This analysis helps to determine the operating conditions of the power plant under minimum fuel cost [40], [41]. In this research, interior point optimization is applied because of its rapid convergence in large power systems and is an effective way of handling large power systems in ETAP software [40]–[50].

There are different types of softwares available for the simulation of models of power systems and power stations. In all of these softwares, ETAP software is found most promising because of its realistic approach and user's control of design and analysis parameters. Therefore, ETAP is associated with many industries for simulation and development [28], [51]–[59].

In this research, a furnace oil-based power plant consisting of more than 160 bus bars of high voltage, medium voltage, and low voltage is designed. Moreover, post-design analyses discussed in the coming section are performed to depict this power plant design performance. This research paper consists of the following sections, Section I covers the introduction and literature review. Section II consists of the methodology involved for the design and analysis of furnace oil-based power plants comprehensively. Section III contains the test system designed for simulation under different scenarios. Section IV consists of a discussion of the results of the simulation. The conclusion is presented in Section V.

2. METHODOLOGY

2.1. Data collection

Relative data for the design of the power plant is gathered. A single line diagram should be provided by the vendor. If collected data is sufficient for the power system studies, then electrical design and analysis program (ETAP) software is used to design a model. If some ratings are not correct or it is not available, the site is visited to gather information. After this, if still data is not sufficient for the model which is collected during the site survey, then assumptions are made based on the different international standards such as IEEE standards, ANSI standards, IEC standards. Different analyses are conducted using ETAP to generate a recommendation report for the power plant. Load flow analysis (LFA) is the first and the foremost technique of system studies. The results of this study further help in the implementation of techniques.

2.2. Load flow analysis

Load flow analysis is the study of power, voltages, and angles at different nodes of bus and specify that whether the system is operating in normal voltages condition or emergency operating conditions, Load flow analysis is performed to design a new power system and modification of the existing system. The voltage (V), voltage angle (δ), real power (P), and reactive power (Q) can be computed using load flow.

Three types of buses are used in load flow which are swing, generator, and load buses. In swing bus, P and Q are found based on and V and δ. In the generator bus, for the input of P and V, the required output of Q and δ is calculated, and in the load bus, P and Q are known and V and δ are unknown values. All the unknown parameters (V, δ, P, and Q) are accessible for swing bus, generator bus, and load bus with load flow analysis. The other electrical parameters such as current, power factor, apparent power for the whole electrical system can be determined based on these four parameters (V, δ, P, and Q) and impedance between the buses (Zij). For the calculation of load flow analysis, there are some methods i.e. Gauss-Seidel method, Newton Raphson method, Adaptive Newton Raphson method. In this research, the Newton Raphson method is implemented because its results are accurate and it requires fewer iterations. Basic model of power system is presented in Figure 1 in which current Ii is entering from the bus (Vi) and is flowing towards different buses (V1, V2, …, Vn) via admittances (yi1, yi2, …, yin).

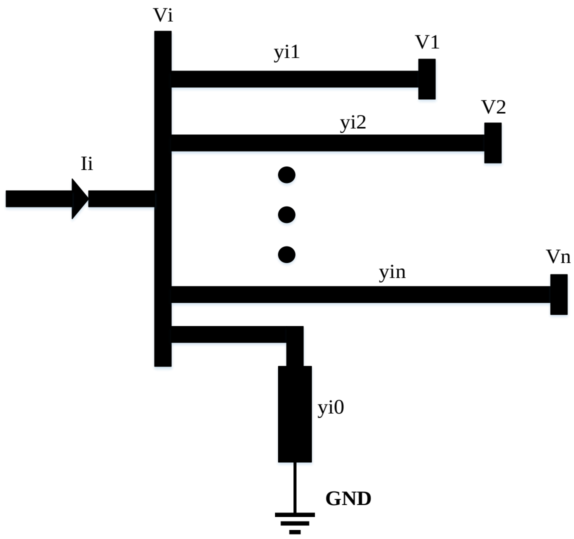

Figure 1. Basic power system

2.2.1. Newton raphson

Newton's method, named after Isaac Newton and Joseph Raphson, is a method for finding successively better approximations to the roots of a real-valued function. The approach to Newton-Raphson load flow is similar to that of solving a system of nonlinear equations using the Newton-Raphson method [4]–[7]. It is an iterative method that approximates a set of non-linear simultaneous equations to a set of linear simultaneous equations using Taylor's series expansion. Referring to Figure 1, power flow equations are formulated in polar form for the n bus system in terms of bus admittance matrix Y as:

$$I_i = \sum_{j=1}^{n} Y_{ij} V_j \tag{1}$$

Where ith and jth buses are donated by i and j. Expressing it in polar form as:

$$I_i = \sum_{j=1}^{n} |Y_{ij}||V_j| < \theta_{ij} + \delta_j \tag{2}$$

The current is expressed in terms of the active and the reactive power at the bus *I* as:

$$I_i = \frac{P_i - jQ_i}{V_i} \tag{3}$$

Substituting for *I*i from (2) in (3) as:

$$\mathrm{P_i - JQ_i = |V_i| < -\delta \textstyle\sum_{i=1} |V_i||V_{IJ}| < \theta_{ij} + \delta_j} \tag{4}$$

Separating the real and imaginary parts as:

$$Pi = \sum_{j=1}^{n} |ViVjYij| \cos(\theta ij + \delta j - \delta i) \quad (5)$$

$$Qi = -\sum_{j=1}^{n} |ViVjYij| \sin(\theta ij + \delta j - \delta i) \quad (6)$$

After expanding (5) and (6) in Taylor's series with initial condition and neglecting higher-order terms as:

$$\begin{bmatrix} \frac{\partial P_2}{\partial \delta_2} & \cdots & \frac{\partial P_2}{\partial \delta_n} & \frac{\partial P_2}{\partial |V_2|} & \cdots & \frac{\partial P_2}{\partial |V_n|} \\ \vdots & \ddots & \vdots & \vdots & \ddots & \vdots \\ \frac{\partial P_n}{\partial \delta_2} & \cdots & \frac{\partial P_n}{\partial \delta_n} & \frac{\partial P_2}{\partial |V_2|} & \cdots & \frac{\partial P_2}{\partial |V_2|} \\ \frac{\partial Q_2}{\partial \delta_2} & \cdots & \frac{\partial Q_2}{\partial \delta_n} & \frac{\partial Q_2}{\partial |V_2|} & \cdots & \frac{\partial Q_2}{\partial |V_n|} \\ \vdots & \ddots & \vdots & \vdots & \ddots & \vdots \\ \frac{\partial Q_n}{\partial \delta_2} & \cdots & \frac{\partial Q_n}{\partial \delta_n} & \frac{\partial Q_n}{\partial |V_2|} & \cdots & \frac{\partial Q_n}{\partial |V_n|} \end{bmatrix} \begin{bmatrix} \Delta\delta_2 \\ \vdots \\ \vdots \\ \Delta\delta_n \\ \Delta|V_2| \\ \vdots \\ \vdots \\ \Delta|V_n| \end{bmatrix} = \begin{bmatrix} \Delta P_2 \\ \vdots \\ \vdots \\ \Delta P_n \\ \Delta Q_n \\ \vdots \\ \vdots \\ \Delta Q_n \end{bmatrix} \quad (7)$$

The Jacobian matrix gives the literalized relationship between small changes in $\Delta\delta_i$ and $\Delta|V_i|$ voltage angle and magnitude with the small changes in real and reactive power ΔP_i and ΔQ_i as:

$$\begin{bmatrix} \Delta P \\ \Delta Q \end{bmatrix} = \begin{bmatrix} J_1 & J_2 \\ J_3 & J_4 \end{bmatrix} \begin{bmatrix} \Delta\delta \\ \Delta|V| \end{bmatrix} \quad (8)$$

The diagonal and the off-diagonal elements of J1 are:

$$\frac{\partial P_i}{\partial \delta_j} = \sum_{j=1}^{n} |ViVjYij| \cos(\theta ij + \delta j - \delta i) \quad (9)$$

$$\frac{\partial Q_i}{\partial \delta_j} = \sum_{j=1}^{n} |VijYij| \sin(\theta ij + \delta j - \delta i) \quad (10)$$

Similarly, the diagonal and off-diagonal elements of J2, J3, and J4 can be evaluated. The terms $\partial P_i{}^k$ and $\partial Q_i{}^k$ are the difference between the scheduled and calculated values, known as the power residuals given as:

$$\Delta P_i^k = P_i^{sch} - P_i^k \quad (11)$$

$$\Delta Q_i^k = Q_i^{sch} - Q_i^k \quad (12)$$

Using the values of the power residuals and the Jacobian matrices, $\Delta\delta_i$ and $\Delta|V_i|$ are calculated from (7) to complete the particular iteration and the new values are calculated as shown below which are used as the initial values for the next iteration.

$$\delta_i^{k+1} = \delta_i^k - \Delta\delta_i^k \quad (13)$$

$$|V_i^{k+1}| = |V_i^k| - |\Delta V_i^k| \quad (14)$$

2.3. Short circuit analysis

Short-circuit studies are performed to determine the peak magnitude of the prospective currents flowing in the power system at different time intervals after a fault occurs. The magnitude of the currents flowing through the power system after a fault varies with time until they reach a steady-state condition. This behavior occurs due to system characteristics and dynamics. During this time, the protective system is called on to detect, interrupt, and isolate this faulty equipment. The duty enforced on this equipment is dependent upon the magnitude of the current, which is dependent on the time from fault inception. This is done for different types of faults (three-phase, phase-to-phase, double-phase-to-ground, and phase-to-ground) at dissimilar locations throughout the system. The information is used to select the size of the equipment like fuses, breakers, and switchgear ratings in addition to setting protective relays.

Motor starting analysis, Motor starting analysis is used to calculate motor acceleration time and the voltage impact on motor starting in electrical power systems. Advanced plotting and time-varying graphical displays enable engineers to quickly evaluate results and to make decisions. In an induction motor, when supply is given to the stator windings, the rotating magnetic field flux, and the produced flux in the rotor windings due to the back emf, cause the motor torque to increase resulting in high rotor current. During the time between the application of electric supply to the motor and the actual acceleration of the motor to its full speed, a large amount of current is drawn by the stator from the supply. This starting current is about 5 to 6 times more than the full load current. This time duration can be for a few milliseconds or longer. This causes the electrical equipment to damage because of the increased voltage drop in electrical systems due to the flow of larger currents across the cable. For this reason, a definite method of starting the motor is needed.

2.4. Transient analysis

The capacity of a power system, containing at least two synchronous machines, to keep on working after a change happened on the system is a check of its stability. The stability issue takes two structures: steady-state and transient. Steady-state security might be characterized as the capacity of a power system to keep up synchronism between machines inside the system following generally moderate load changes. Transient stability is the virtue of the system to stay in synchronism under transient conditions, i.e., abnormal and switching operation, etc. In a modern power system, stability may include the power organization system and at least one in-plant generator or synchronous machine. Following are the possibilities i.e., for example, load dismissal, unexpected loss of a generator or utility tie, starting of motors or fault (and their time interval), directly affect system stability and efficiency. Load-shedding schemes and basic flaw clearing times can be resolved to choose the best possible settings for protection relays. These kinds of studies are likely the absolute most complex ones done on a power system. The beginning stage for any transient stability simulation is the pre-disturbance control power flow arrangement. The system is constantly thought to be in a consistent state when the aggravation happens. Utilizing the pre-disturbance power flow solution, all the underlying estimations of the state factors are determined after these are acquired, the disturbance is simulated. The simulation of the disturbance causes a conflict between the mechanical power contribution to the generators and the electrical power yield of the generators. The equilibrium is disturbed. The state factors calculated by the different differential conditions combined with mathematical conditions change their values. A transient stability study has been done by introducing a three-phase and L-G fault and its clearance on different buses. The system is analyzed under the transient produced by these abnormal conditions. The system generator's reaction at beginning of this issue and clearance of this disturbance has been recorded.

2.5. Economic dispatch

Due to the increasing price of fuel oil, wages, and salaries, the electrical energy cost also increases, so one should keep in mind the cost factor while operating or building a new power system, to meet the growing load demand. In the operation of the power system, the contribution from each load and each unit within a plant must be such that the cost of electrical energy produced is minimum. Interior point optimization is the technique through economic dispatch is conducted in ETAP.

The reduction of generation cost is called economic dispatch as shown in Figure 2. In the generation, cost includes the operational cost, maintenance, labor, and supply cost. Mostly, the generation cost is present as quadratic of input fuel and power generation cost in economic dispatch and other constraints are voltage limits, real and reactive power limits, and power balance condition [40]–[45]. To understand the economic dispatch, a problem is presented in the mathematical description as:

$$Min \sum_{i=1}^{NG} (\alpha_i + \beta_i P_{Gi} + \gamma_i P_{Gi}^2)$$

Subject to:

$$\sum_{i=1}^{NG} (P_{Gi}) = P_D + P_L \tag{15}$$

$$P_{Gi}^{min} \leq P_{Gi} \leq P_{Gi}^{max}$$

Where α, β, and γ are the parameters that are dependent on the system and they affect real generation power cost. The total number of generators is represented by NG. P_i is the real power generation at bus i and P_D and P_L are total power demand and power losses in the power transmission network respectively. The quadratic interior-point program converts economic dispatch problem in the following format [46]–[50]:

$$Min\ (A^T E + \bar{B}^T x + \frac{1}{2} x^T \bar{Q} x)$$

Subject to

$$b^{min} \leq Ax \leq b^{max} \tag{16}$$

$$F(x) = 0$$

Where $x = (P_{G1}, \dots\dots, P_{GNG}, P_{Gs1}, \dots., P_{Gs2NG})^T$, $E = (1, \dots.,1)^T$, $A = (\alpha_1, \dots, \alpha_{NG}, 0, \dots,0)^T$, $B = (\beta_1, \dots, \beta_{NG}, 0, \dots,0)^T$ and,

$$\bar{Q} = \begin{bmatrix} q_{11} & & & & & \\ & \dots & & & & \\ & & q_{NG,NG} & & & \\ & & & 0 & & \\ & & & & \dots & \\ & & & & & 0 \end{bmatrix} \quad (17)$$

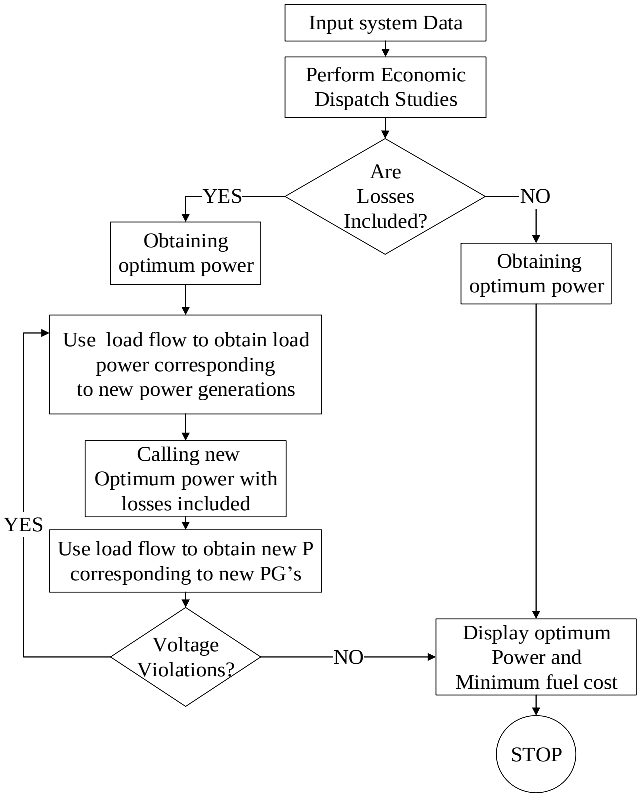

Figure 2. Proposed flow chart of inter-point optimization for economic dispatch

3. TEST SYSTEM

The test system is composed of three main sections which are described below. It contains nine furnace oil-based generators and one combined cycle-based generator. Further detail is followed by each section.

3.1. High voltage side

The high voltage side is composed of two main buses which are directly fed from two utility buses as given in Figure 3. These buses have a 132 KV nominal voltage level.

3.2. Medium voltage side

Voltages are stepped down from 132 to 15 KV for connecting it to generators as shown in Figure 4. The medium voltage side is composed of three main generator buses. Gen bus-1and Gen bus-2 are fed from generators 1,2,3,4 and generators 5,6,7,8 respectively. Each generator has a rated capacity of 17500 KW. Every generator bus is linked with each other using a bus coupler to maintain the supply in case of any fault. Gen bus-3 is connected directly to Generators 9 and 10. Gen 9 and 10 have rated capacity of 17500 and 10750 kW respectively. Now again, voltage levels are stepped down to 0.415 KV for supplying to the LV side.

3.3. Low voltage side

Low voltage is modeled by using a composite network for avoiding the complexity in the case of a large-scale power network. As explained before, low voltage side buses have a nominal voltage level of 0.415 kV. This section is consisting of three feeders as shown in Figure 5, Figure 6 and Figure 7.

Each feeder is further composed of sub-buses. These buses are attached to the auxiliary loads required for operating the whole power unit. Auxiliary loads have a long list of loads. So, the loads are lumped on LV buses depending upon their rated kW. All the loads which are less than 30 kW are lumped while modeling on ETAP.

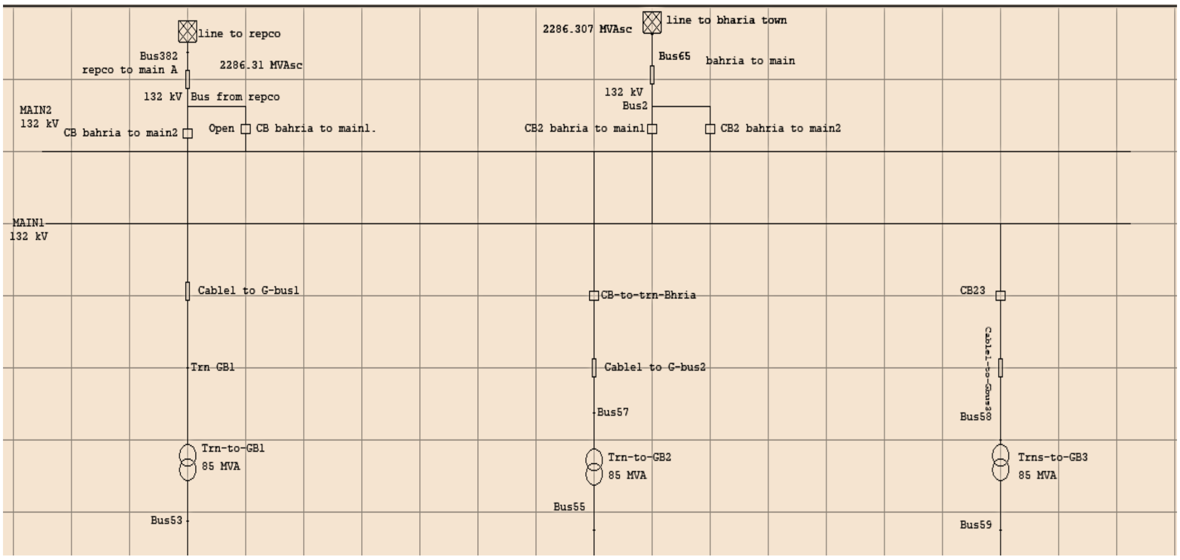

Figure 3. A sectional view of high voltage side

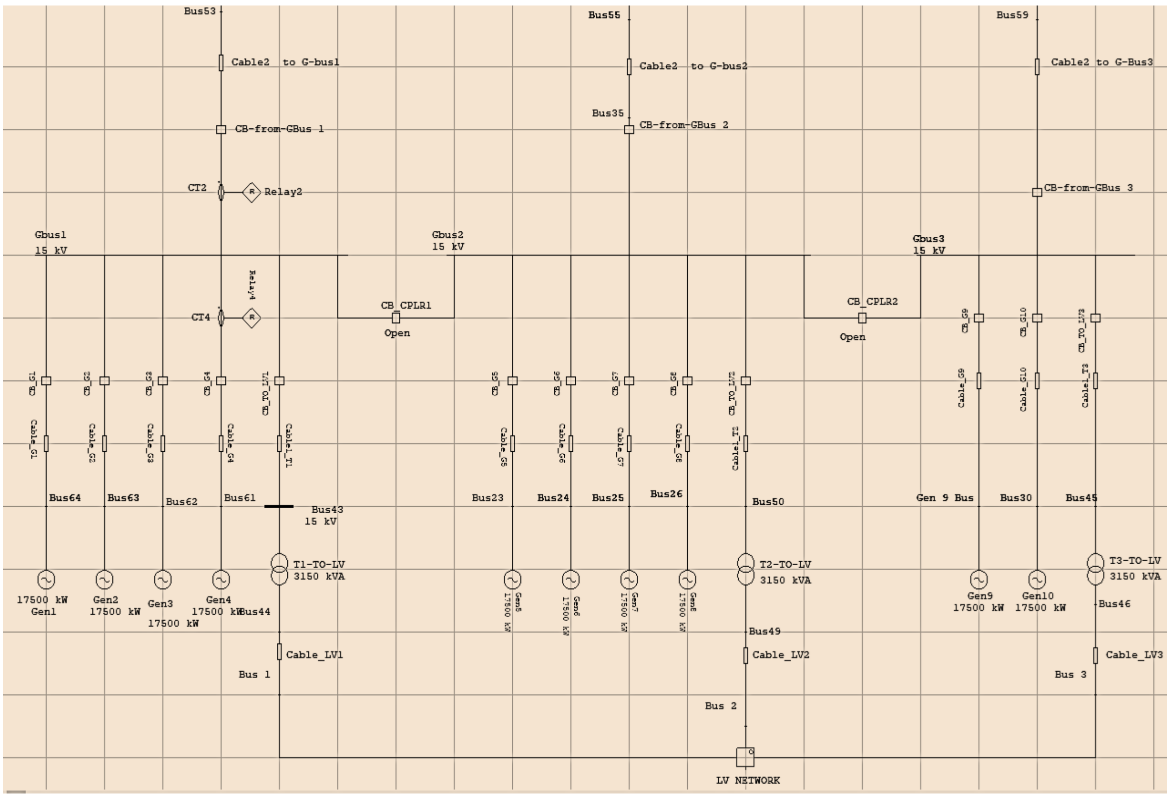

Figure 4. A sectional view of medium voltage side

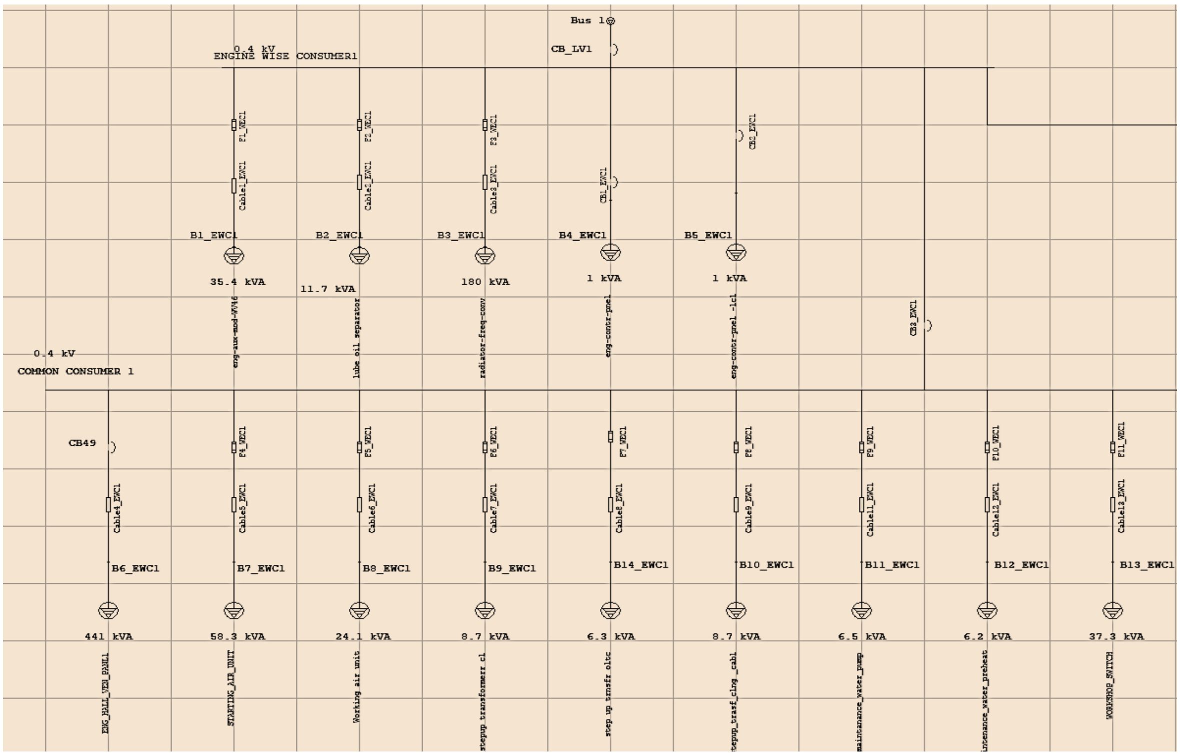

Figure 5. A sectional view of low voltage side feeder 1

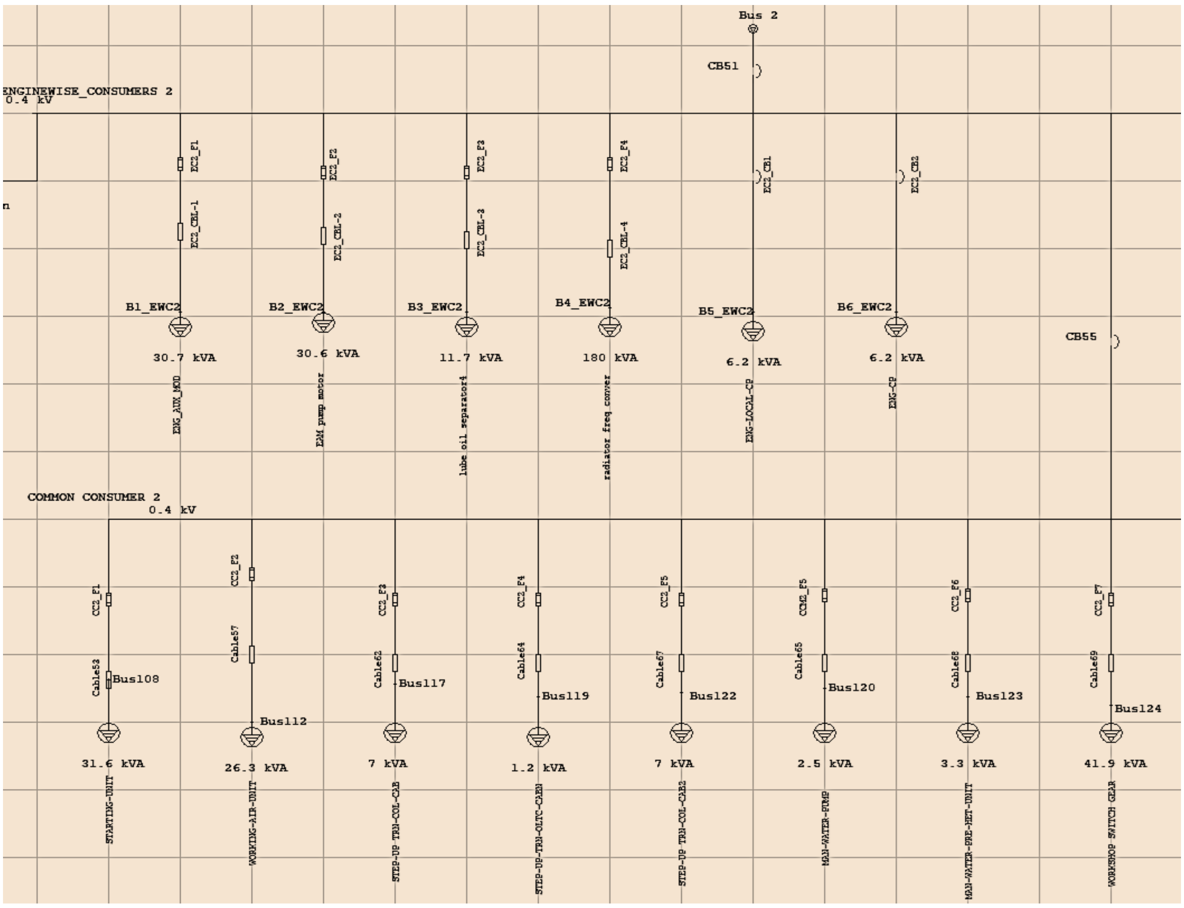

Figure 6. A sectional view of low voltage side feeder 2

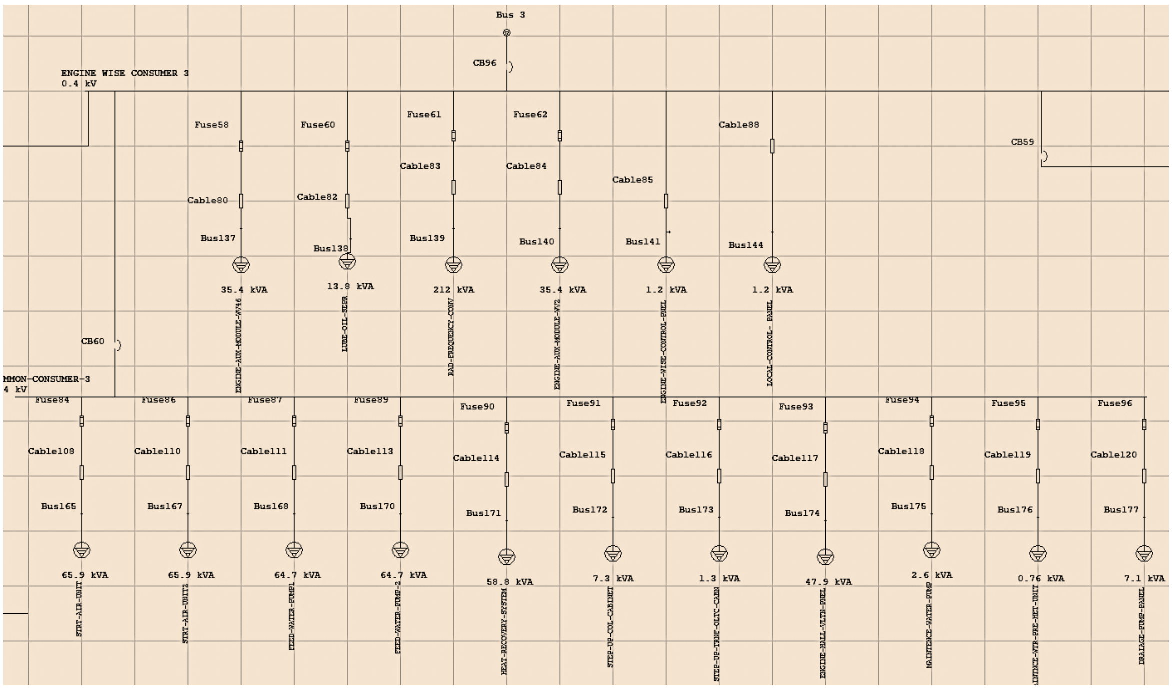

Figure 7. A sectional view of low voltage feeder 3

4. SIMULATION RESULTS

4.1. Load flow analysis

A load flow calculation determines the state of the power system for a given load and the distribution of generation. It represents a steady-state condition as if that condition has been held fixed for some time. In reality, power flows and bus voltages fluctuate constantly by small amounts because loads change constantly as lights, motors, cooling equipment, and other loads are turned on and off. However, these small fluctuations can be ignored in calculating the steady-state effects on system equipment. Load flow study is performed on the basis and recommendations of the following international standards: IEEE STD 399-1997. (IEEE recommended practice for industrial and commercial power system analysis) and IEEE STD 141-1993 (IEEE recommended practice for electric power distribution for industrial plants). After performing load flow, voltages at each bus are checked which should be under safe level as shown in Table 1.

Table 1. Percentage loading on each bus

Bus	Nominal Voltage (kV)	Voltage (%)	Nominal Current (A)	Loading (A)	% Loading
MAIN-1	132	100	2000	402.3	20.1
MAIN-2	132	100	2000	342.8	17.1
G-BUS1	15	105.86	3600	2532	70.3
G-BUS2	15	105.85	3600	2531	70.3
G-BUS3	15	102.96	3600	1085	30.1
ENG-WISE-CONNSUMER1	0.4	104.79	5000	1567	31.3
ENG-WISE-CONNSUMER2	0.4	103.23	5000	1429	28.6
ENG-WISE-CONNSUMER3	0.4	97.79	5000	1578	31.6

Figure 8 explains the graph between the nominal and actual voltage on different buses. As it is seen that loading at main1and main 2 buses are within the limits of 95-105% so it depicts that all the buses are sized properly. Figure 9 graph between the maximum withstands capacity of buses for short circuit fault and actual fault current flowing through the buses. All the buses have a fault current that is lesser than the maximum withstand capacity of the buses. For example; G bus1 and G bus 2 have fault current of 2.531 kA and 1.0835 kA respectively and their maximum withstands capacity are 3.6 kA respectively.

Figure 10 is the graph between the rated power and actual active power of each generator at a constant power factor. As it is seen from the graph that Gen 7 and steam turbine generator have rated active power of 17.5 MW and 10.75 MW respectively where their actual active power is 16 MW and 9 MW respectively. One thing that is noted is that the required MW is attainable from the generators at a power factor of 0.85. Table 2 covers the details of rated active power (KW) and rated reactive power (KVAR) of each generator.

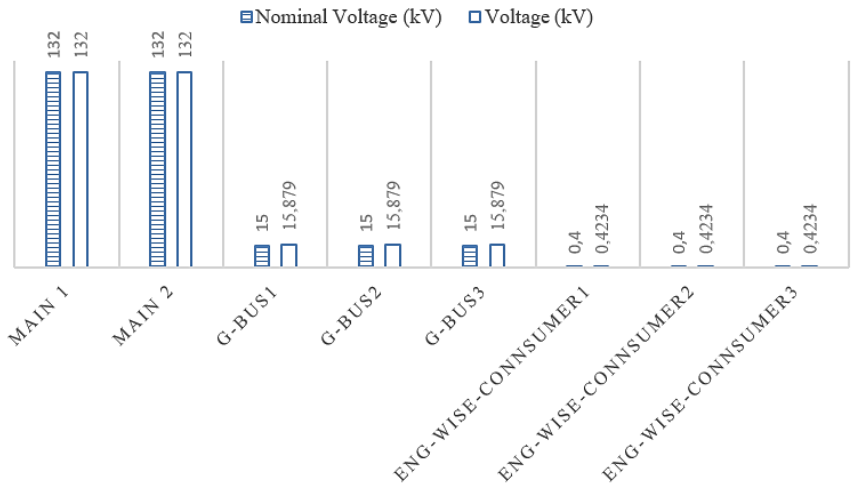

Figure 8. The graph between the nominal and actual voltage on different buses

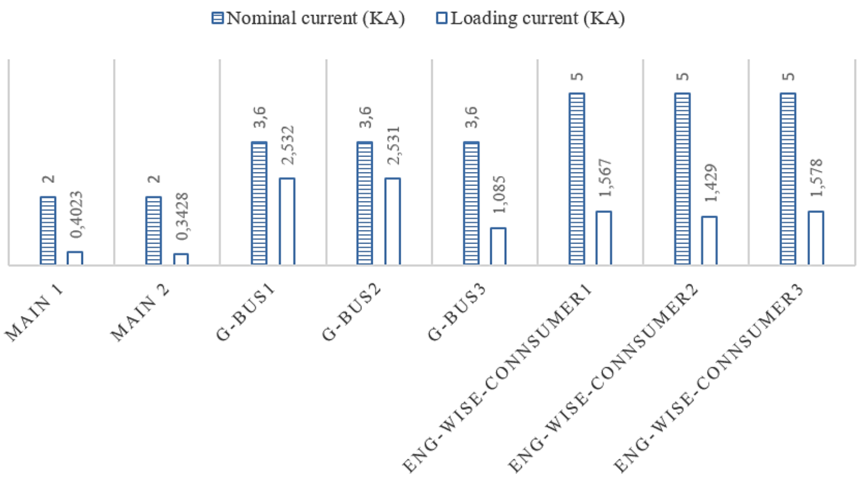

Figure 9. Graph between nominal and loading current of different buses

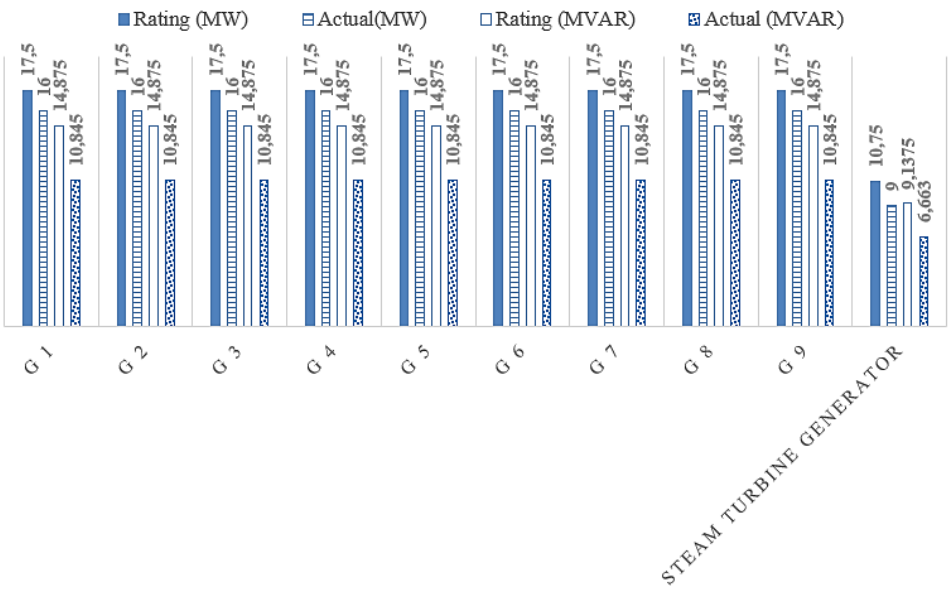

Figure 10. Graph of generator between rated and actual real and reactive power

Table 2. Rated KW and KVAR of each generator

Generators	Nominal Voltage (kV)	Rating (kW)	KW	KVAR	% PF	%Generation
G 1	15	17500	16000	10845	85	100
G 2	15	17500	16000	10845	85	100
G 3	15	17500	16000	10845	85	100
G 4	15	17500	16000	10845	85	100
G 5	15	17500	16000	10845	85	100
G 6	15	17500	16000	10845	85	100
G 7	15	17500	16000	10845	85	100
G 8	15	17500	16000	10845	85	100
G 9	15	17500	16000	10845	85	100
Steam Turbine Generator	15	10750	9000	6663	85	75.8

4.2. Short circuit analysis

The graph depicts the relationship between short circuit current, three-phase fault current, the line to ground, line to line current with respect to the maximum withstand capacity of each bus. As seen from Figure 11 that at Gbus-3, three-phase device duty, a line to ground, and line to line faults have the values of 35.1, 30.74, and 30.58 KA respectively. The maximum withstand capacity of G bus-3 is 40KA as shown in Figure 11. So, from the observations, it is concluded that the different fault values exist at different buses. Based on these values, the protection scheme for the tested system is designed.

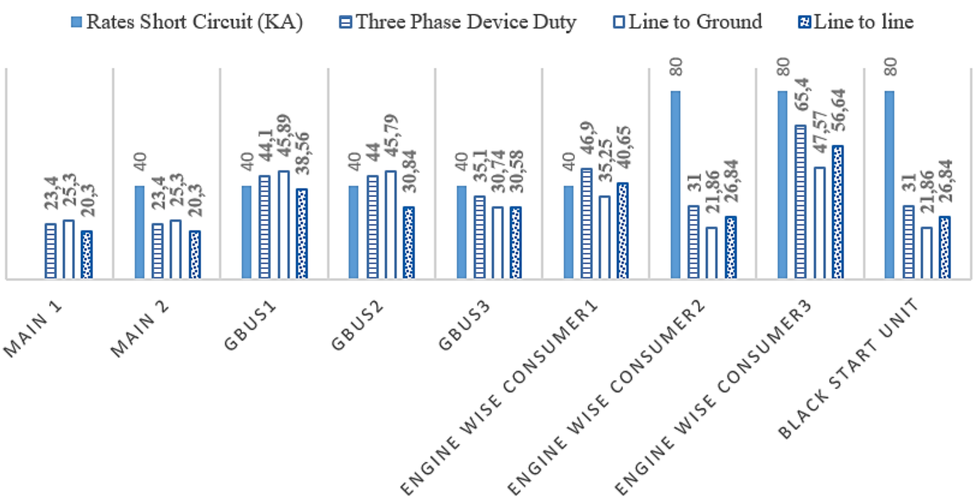

Figure 11. Graph of short circuit current, three-phase fault current, the line to ground, line to line current

4.3. Motor starting analysis

The test system is analyzed by starting the biggest motor of the system and its effects on all the buses are observed and are presented in Table 3. This motor is connected with the black start unit bus. After performing motor starting analysis, all the profiles are checked with respect to the time which is within the safe limits. Voltage dip is seen from the graph on the black start unit bus. The graph shown in Figure 12 explains the variation in voltage at different buses with respect to time.

It is seen from the graph that at t=1sec, the motor starts and there is seen a voltage dip at Main 1 and Main 2 which is 131.986 KV when the nominal voltages on both buses are 132 KV as shown in Figure 12. There is a voltage dip 0.2 KV at the main bus. It is also seen from the graph that after few seconds, voltage again retains its normal value which is 132 KV. It is concluded that voltage drop is within the marginal limits which are followed internationally for the motor starting purpose. It is noted that motor starting analysis is done with the respect to 50 kW motor starting at black start unit bus. Figure 13 shows the ETAP generated graph of bus voltage with respect to time. At the black start unit bus, there is a voltage dip at 1 second when the motor starts and after some time voltage again retains to its level. All the other buses have no dip because the corresponding motor is connected to the black start unit only.

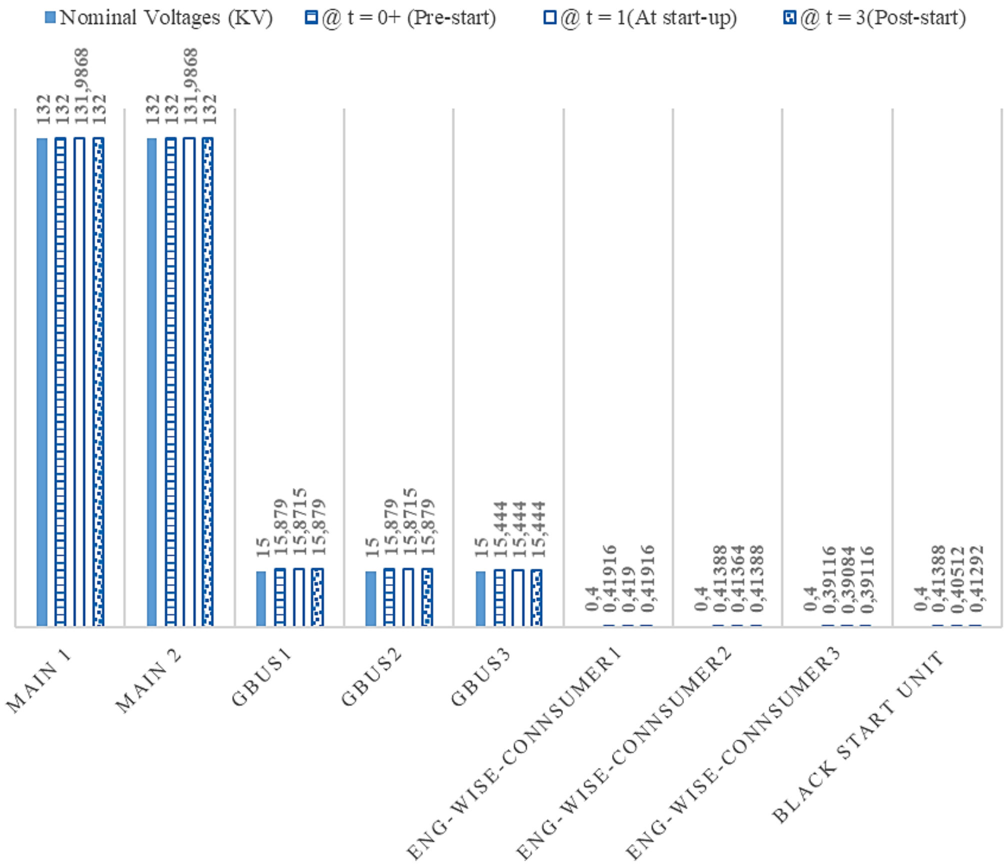

Figure 12. Graph of variation in voltage at different buses with respect to time

Table 3. Voltage profiles at various intervals analyzed during motor starting analysis

Bus	Nominal Voltage (kV)	Voltage profile (%) at various time intervals (Seconds)		
		@ t = 0+ (Pre-start)	*@ t = 1(At start-up)*	*@t=3(Post-start)*
MAIN 1	132	100	99.99	100
MAIN 2	132	100	99.99	100
Gbus1	15	105.86	105.81	105.86
Gbus2	15	105.86	105.81	105.86
Gbus3	15	102.96	102.96	102.96
Eng-Wise-Connsumer1	0.4	104.79	104.75	104.79
Eng-Wise-Connsumer2	0.4	103.47	103.41	103.47
Eng-Wise-Connsumer3	0.4	97.79	97.71	97.79
Black start unit	0.4	103.47	101.28	103.23

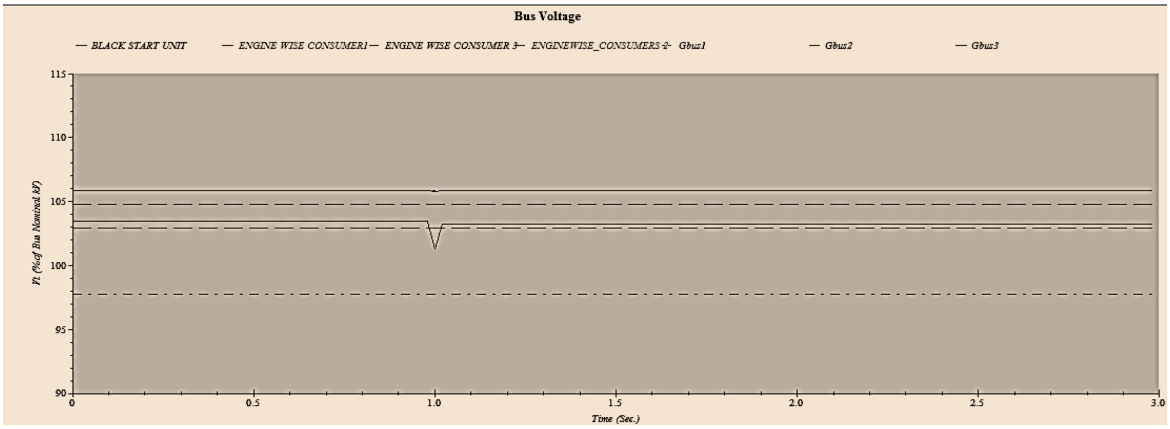

Figure 13. ETAP generated a graph of bus voltage with respect to time

4.4. Transient stability analysis

Transient analysis is performed under two cases. kW, kVAR, Terminal current, Speed, and other parameters of generators (presented in Figure 14) are analyzed.

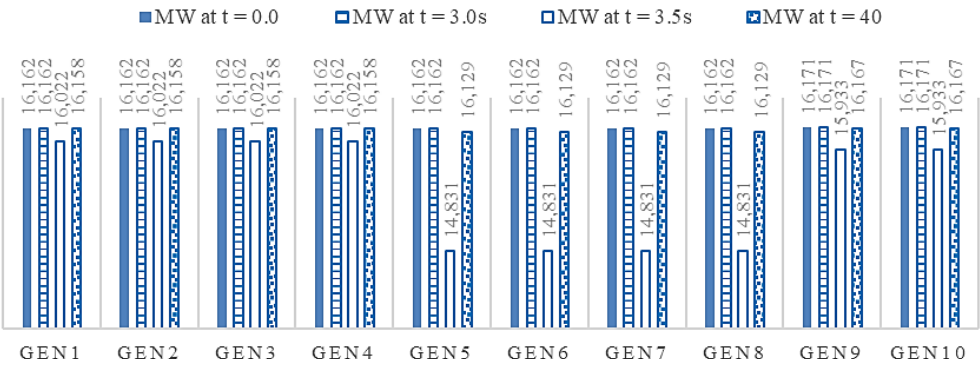

Figure 14. Graph of generated MW of different generators with respect to time

a. Case Sc-GB

In this case, a three-phase fault is introduced on generator bus 2 and is cleared after some interval. Figure 14 shows the graph of generated MW of different generators with respect to time. It is seen that at Gen1 and Gen2. At t=0 and t=3, the active power is 161.32 MW which remains constant when a transient is induced on the generator at bus 2. Figure 15 shows the Graph of reactive power with respect to time. It is easily cleared from the graph that at reactive power of generators 7 and 9 have transient at t=3sec. After some time, the transient is again normalized to the level before the transient. It is seen that the transient time is in the constraint which is internationally followed. Figure 16 is the graph of terminal current with the variation in time. It is seen from the graph at t=3sec generator 9 have a large terminal current with respect to the other generator such as generator 2,3and 4. Gen 9 terminal current is 3000A and generators 2, 3, and 4 have terminal currents of 500A respectively. When a three-phase fault is introduced on G-Bus2, then the system will operate in a transient state as seen in Figure 17. Voltage dip is seen at the G-buses. This abnormal condition is settled in some period of time and the operation of the generator also becomes normal.

In transient conditions, all other parameters are disturbed but there is a significant effect of transient conditions on generators MW. As seen in Figure 18, MW of Gen-9 is raised to a very high value of 50 MW as compared to the other generators. It is noticed that the effect of transient is more prominent on Gen -9 with respect to the other generators but the value will remain in considerable range. A protection system will correspond to these types of transient very efficiently. This attribute will increase the reliability of the system.

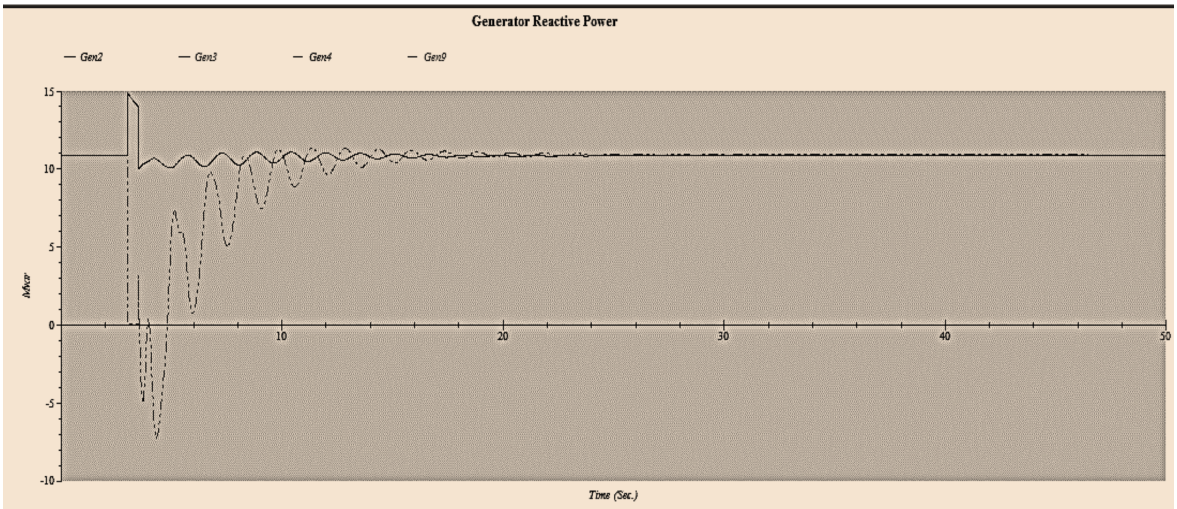

Figure 15. This ETAP-generated graph is between MVAR and time

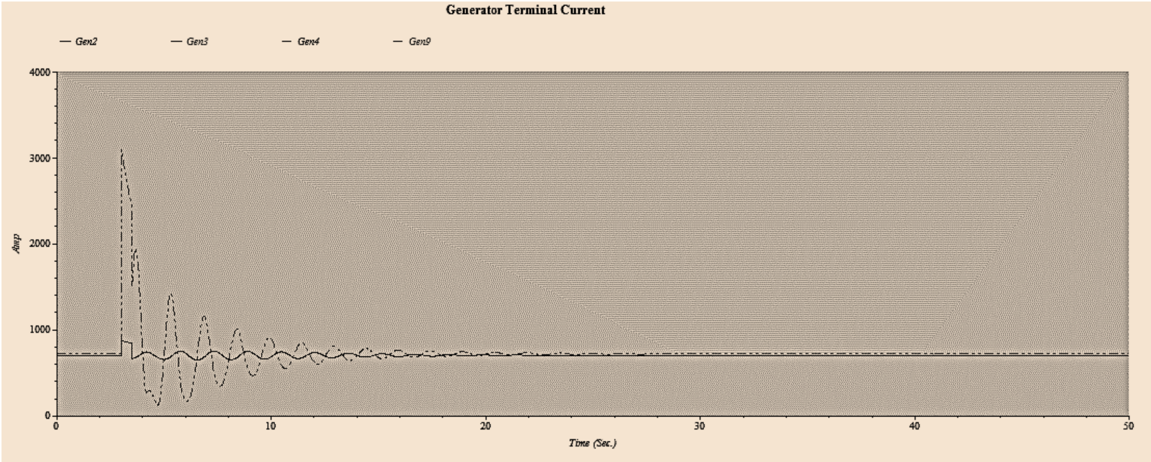

Figure 16. This is the plot of the generator terminal current with respect to time

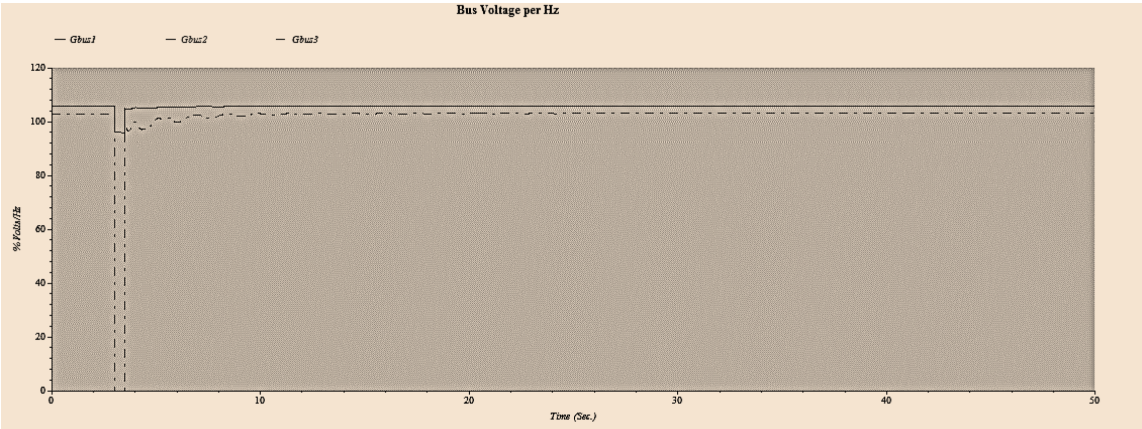

Figure 17. Bus voltage with respect to time when transient case 1 exists

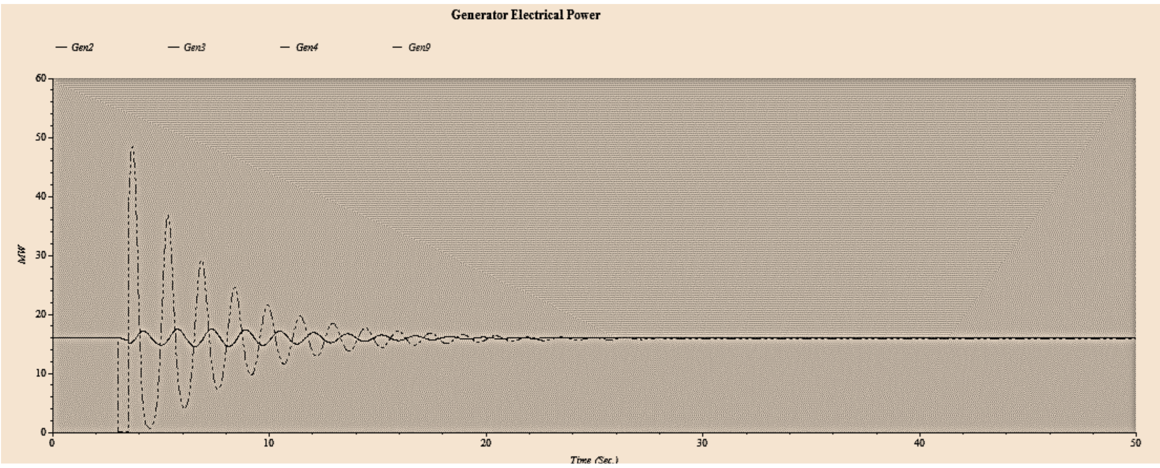

Figure 18. This figure shows the generator's MW with respect to time

b. Case Sc-GB2

In this case, a line to ground fault is introduced at generator bus2 and removed after some interval. After some observation and working on the tested system, a comparison is established with respect to the time of transient case-2. In transient case-2, a line to ground fault is induced on G-bus 2. As shown in Figure 19, at t=3.5 seconds, Gen 9 has an active power rating of 2.034 MW which is a huge variation. This behavior illustrates the effect of transients very clearly. Figure 20 shows the transient stability in terms of rated active power (MW). Stability is achieved in 30 seconds. In 20 seconds, transient stability is achieved in term of rated reactive power (MVAR) as shown in Figure 21. Rate of change of active power and reactive power ultimately affect the current and voltage. Therefore, under transient stability analysis, current and voltage study are also done and is presented in Figure 22 and Figure 23.

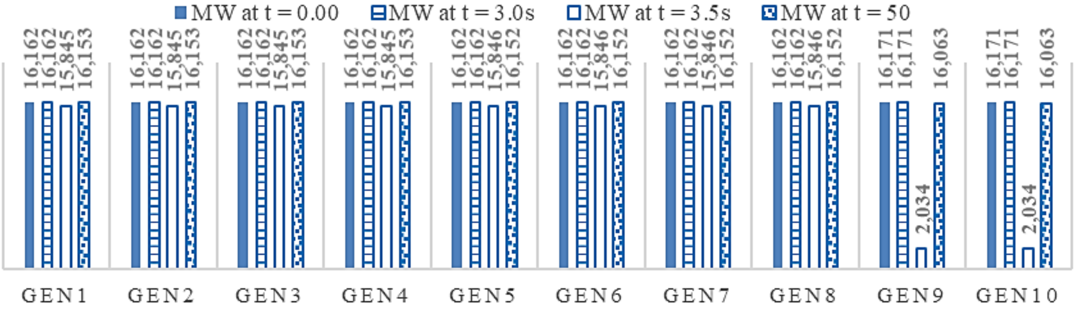

Figure 19. Graph of generated MW of different generators with respect to time

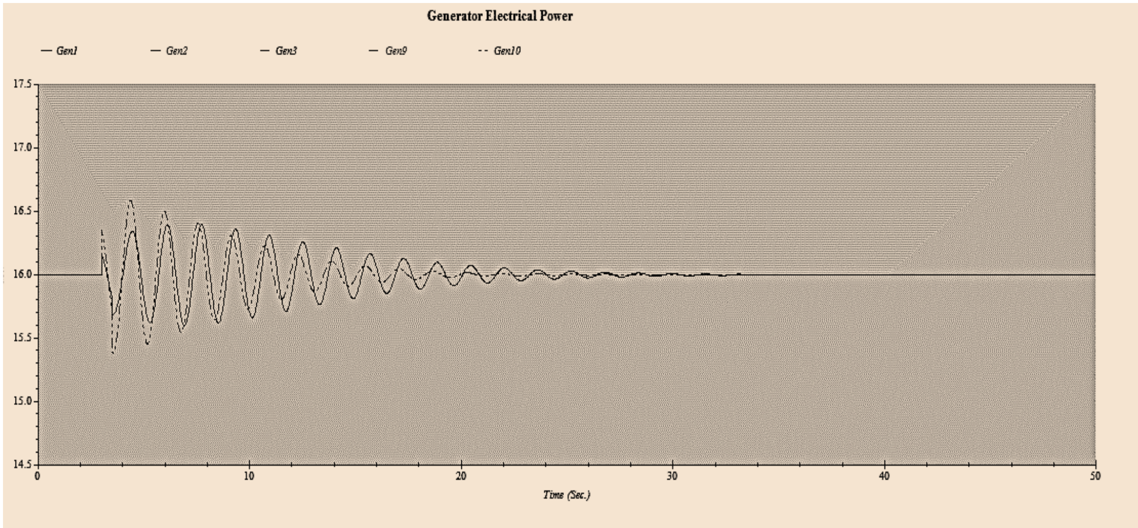

Figure 20. This is the plot of MW with respect to time in transient case-2

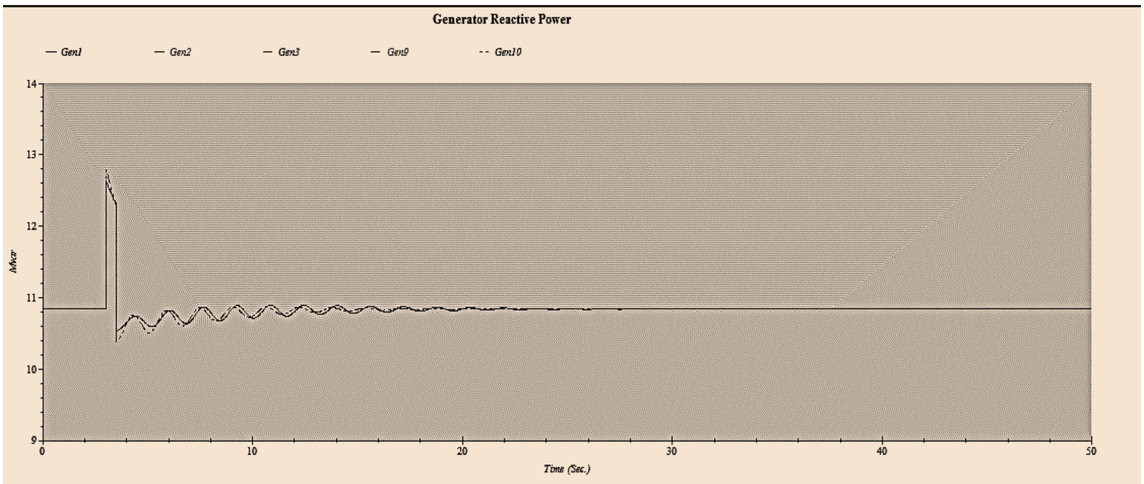

Figure 21. This is the plot of MVAR and time in transient case 2

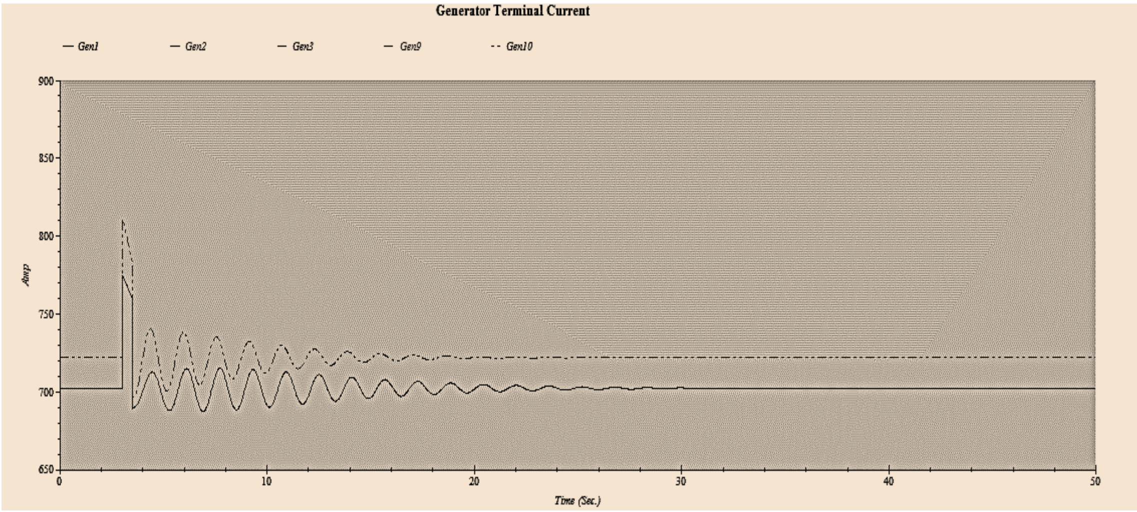

Figure 22. This is the graph of generator terminal current and time in transient case 2

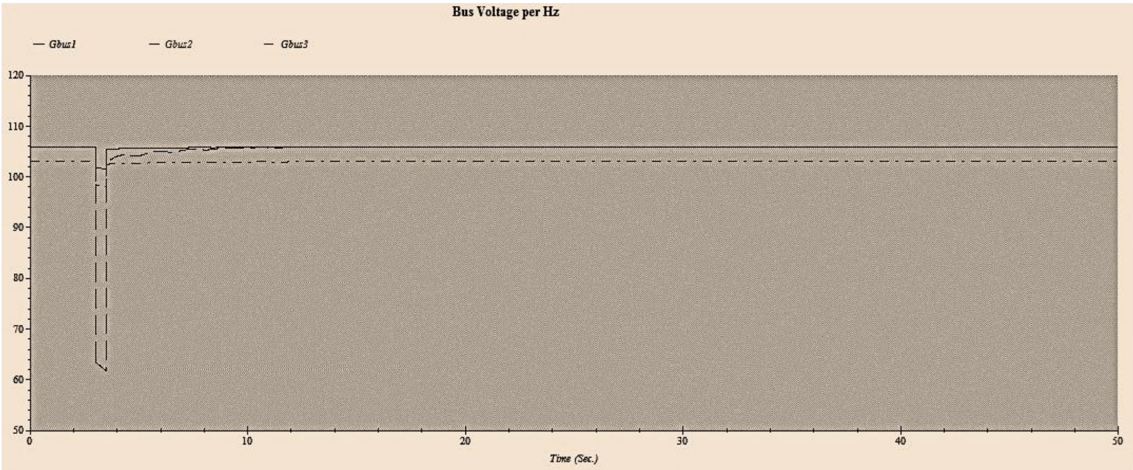

Figure 23. This is the graph between bus voltages and time in transient case 2

4.5. Economic dispatch

In the end economic dispatch of the tested power system is done using the optimal load flow module of ETAP as shown in Figure 24. Optimal load flow ensures the usage of maximum power with the variable amount of constraint which could be varied according to the different priorities and scenarios. Economic dispatch study is performed in a larger network where a furnace-based power plant was generating electricity along with a coal-fired and a hydropower plant. It appears from the study that it is economically optimum to utilize a furnace oil-based power plant at 56.7% of its total capacity. This also emphasizes the need to utilize furnace oil power plants even though cheaper fuel power plants are present in the system.

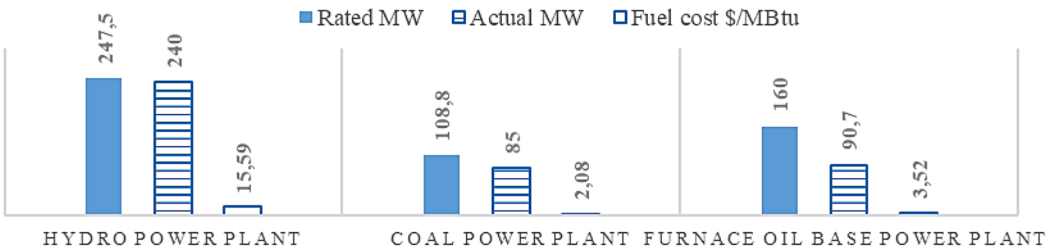

Figure 24. The graph between the cost of different fuels wrt to the MW at simple and optimum load flow

5. CONCLUSION

Growing demands of energy can only be fulfilled with the addition of new power generating units and modification of existing power generating systems. In addition to this, there is a need to look up new energy sources to meet the energy requirement in an optimum way. In this comprehensive research, a furnace oil-based power plant is developed and analyzed under different pre-design and post-design analyses so that recommendations could be prepared under international standards. Therefore, load flow analysis, short circuit analysis, motor starting analysis, and transient analysis are conducted to depict the practical feasibility of equipment involved in the design of furnace oil-based power stations. Because of conducting simulations under IEEE standards, a very practical approach is followed. In addition to this, ETAP also adds fuel to this research because of its practical viability. Economic dispatch is also performed to find out the optimum rating capacity of a power plant with minimum fuel cost in an interconnected system. The compatibility of this research with

ACKNOWLEDGEMENTS

The authors are thankful to the Department of Electrical Engineering, University of Lahore, Lahore, Pakistan, for providing facilities to study power stations using ETAP simulations.

REFERENCES

[1] A. H. Abbasi, F. Mahmood, M. Kamal, and A. Baig, "Pakistan Energy Vision - 2035," *Sustainable Development Policy Institute (SDPI), Pakistan, Information*, 2022. [Online]. Available: https://thecoalhub.com/wp-content/uploads/2018/12/Pakistan-Energy-2035-FINAL-20th-October-2014.pdf

[2] T. Gonen, "*Electric Power Transmission System Engineering Analysis and Design*, " Third. Boca Raton: CRC PRESS, 2015.

[3] R. Owen, "One Hundred Years of Middle Eastern Oil," *Middle East Brief*, vol. 24, pp. 1-6, 2008.

[4] R. Muzzammel, M. Ahsan, and W. Ahmad, "Non-linear analytic approaches of power flow analysis and voltage profile improvement," *Power Generation System and Renewable Energy Technologies (PGSRET)*, pp. 1–7, 2015, doi: 10.1109/PGSRET.2015.7312232.

[5] J. J. Grainger, W. D. Stevenson, and W. D. Stevenson, "*Power system analysis*," New York: McGraw-Hill, 1994.

[6] H. Saadat, "*Power system analysis*," United States: PSA Pub., 2010.

[7] D. P. Kothari and I. J. Nagrath, "Modern power system analysis," *Fourth edition. Chennai: McGraw Hill Education (India) Private Limited*, 2011.

[8] S. Chatterjee and S. Mandal, "A novel comparison of gauss-seidel and newton- raphson methods for load flow analysis," *International Conference on Power and Embedded Drive Control (ICPEDC)*, Chennai, India, Mar. 2017, pp. 1–7. doi: 10.1109/ICPEDC.2017.8081050.

[9] A. N. Afandi, I. Fadlika, and L. Gumilar, "Power Flow Analysis of Power System Topology Development for Advancing Electricity System of Local Interconnection," *4th International Conference on Science and Technology (ICST)*, Yogyakarta, Aug. 2018, pp. 1–6. doi: 10.1109/ICSTC.2018.8528690.

[10] M. N. Malik, A. I. Toor, M. A. Siddique, N. Hussain, and A. Nadeem, "Load flow analysis of an EHT network using ETAP," *Journal of Multidisciplinary Engineering Science and Technology*, vol. 3, no. 6, pp. 4979–4984, 2016.

[11] P. Raj, "Load flow and short circuit analysis of 400/220 kV substation," *International Journal of Creative Research Thoughts*, vol. 1, no. 4, pp. 1–4, 2013.

[12] R. Muzzammel, M. N. Akram, S. Asghar, A. Saleem, and U. Muqeem, "Simulation Analysis of Fully Protected Induction Motor," *International Journal of Scientific & Engineering Research*, vol. 9, no. 10, pp. 770–775, 2018.

[13] R. Muzzammel, I. Khail, M. H. Tariq, A. M. Asghar, and A. Hassan, "Design and Power Flow Analysis of Electrical System Using Electrical Transient and Program Software," *Energy and Power Engineering*, vol. 11, no. 4, pp. 186–199, 2019, doi: 10.4236/epe.2019.114011.

[14] R. Muzzammel, R. Arshad, S. Mehmood, and D. Khan, "Advanced energy management system with the incorporation of novel security features," *International Journal of Electrical and Computer Engineering*, vol. 10, no. 4, pp. 3978-3987, Aug. 2020, doi: 10.11591/ijece.v10i4.pp3978-3987.

[15] M. Raheel and A. Haroon, "Monte Carlo Simulation of Load Flow Analysis of Power System," *International Journal of Scientific & Engineering Research*, vol. 8, no. 3, pp. 534–537, 2017.

[16] "Sihanoukville Combined Cycle Power Development Project," *Japan International Cooperation Agency (JICA), Japan, Technical Report 11675089_02*, 2014. [Online]. Available: https://openjicareport.jica.go.jp/pdf/11675089_02.pdf

[17] B. Patil and S. Namekar, "Load Flow & Short Circuit Analysis of 132/33/11KV Substation using ETAP," *International Journal of Applied Engineering Research*, vol. 13, no. 11, pp. 9943–9952, 2018.

[18] A. Zeggai and F. Benhamida, "Power flow and Short circuit of 220 kV Substation using ETAP," *Algerian Large Electrical Network Conference (CAGRE)*, Algeria, 2019, pp. 1–6. doi: 10.1109/CAGRE.2019.8713172.

[19] K. V. Natkar and N. Kumar, "Short Circuit Analysis Of 220/132 kV Substation By Using ETAP," *International Journal of Advanced Technology in Engineering and Science*, vol. 4, no. 3, pp. 122-129, 2016.

[20] P. S. Patil and K. B. Porate, "Starting Analysis of Induction Motor: A Computer Simulation by Etap Power Station," *Second International Conference on Emerging Trends in Engineering & Technology*, Nagpur, India, 2009, pp. 494–499. doi: 10.1109/ICETET.2009.211.

[21] Y. Youxin, X. Zezhong, W. Yalan, Y. Peigang, and P. Wanquan, "A Soft Starter of Three Phase Asynchronous Motor," *IEEE Power Electronics Specialists Conference*, Orlando, FL, USA, 2007, pp. 563–567. doi: 10.1109/PESC.2007.4342049.

[22] F. Harashima, "Power electronics and motion control-a future perspective," *Proceedings of the IEEE*, vol. 82, no. 8, pp. 1107–1111, 1994, doi: 10.1109/5.301679.

[23] H. Zhu, X. Liu, and N. E. Mastorakis, "The Simulation Analysis of Motor Startup Based on the ETAP Platform," *International Conference on Mathematics and Computers in Sciences and in Industry*, Varna, 2014, pp. 245–248. doi: 10.1109/MCSI.2014.36.

[24] A. R. Bergen and D. J. Hill, "A Structure Preserving Model for Power System Stability Analysis," *IEEE Transactions on Power Apparatus and Systems*, vol. PAS-100, no. 1, pp. 25–35, 1981, doi: 10.1109/TPAS.1981.316883.
[25] J. Geeganage, U. D. Annakkage, T. Weekes, and B. A. Archer, "Application of Energy-Based Power System Features for Dynamic Security Assessment," *IEEE Transactions on Power Systems*, vol. 30, no. 4, pp. 1957–1965, 2015, doi: 10.1109/TPWRS.2014.2353048.
[26] W. Xu, "Status and future directions of power system harmonic analysis," *IEEE Power Engineering Society General Meeting*, Denver, CO, USA, 2004, vol. 2, pp. 756–761. doi: 10.1109/PES.2004.1372917.
[27] E. Acha, "FACTS: modelling and simulation in power networks," *Chichester: Wiley*, 2010.
[28] K. Brown, F. Shokooh, H. Abcede, and G. Donner, "Interactive simulation of power systems: ETAP applications and techniques," *Conference Record of the 1990 IEEE Industry Applications Society Annual Meeting*, Seattle, WA, USA, 1990, pp. 1930–1941. doi: 10.1109/IAS.1990.152451.
[29] A. J. Williams and M. S. Griffith, "Evaluating the Effects of Motor Starting on Industrial and Commercial Power Systems," *IEEE Transactions on Industry Applications*, vol. IA-14, no. 4, pp. 292–305, 1978, doi: 10.1109/TIA.1978.4503541.
[30] Task Force on Blackout Experience, Mitigation, and Role of New Technologies, "Blackout Experiences and Lessons, Best Practices for System Dynamic Performance, and the Role of New Technologies," *Power System Dynamic Performance Committee*, 2007.
[31] X. Luo, J. Wang, M. Dooner, and J. Clarke, "Overview of current development in electrical energy storage technologies and the application potential in power system operation," *Applied Energy*, vol. 137, pp. 511–536, 2015, doi: 10.1016/j.apenergy.2014.09.081.
[32] J. Machowski, Z. Lubosny, J. W. Bialek, and J. R. Bumby, "Power system dynamics: stability and control," Third edition. Hoboken, NJ, USA: John Wiley, 2020.
[33] S. Lozano, L. Buzna, and A. D. Guilera, "Role of network topology in the synchronization of power systems," *The European Physical Journal B*, vol. 85, no. 7, p. 231, 2012, doi: 10.1140/epjb/e2012-30209-9.
[34] P. W. Sauer and M. A. Pa*i*, "Power system dynamics and stability," Upper Saddle River, N.J: Prentice Hall, 1998.
[35] H.-D. Chiang, "*Direct Methods for Stability Analysis of Electric Power Systems: Theoretical Foundation*," *BCU Methodologies, and Applications*. Hoboken, NJ, USA: John Wiley & Sons, Inc., 2010. doi: 10.1002/9780470872130.
[36] P. Kundur, N. J. Balu, and M. G. Lauby, "Power system stability and control," New York: McGraw-Hill, 1994.
[37] K. R. Padiyar, *Power system dynamics: stability and control*, Second edition. Tunbridge Wells: Anshan, 2004.
[38] D. S. Reddy and Ch. S. Kumari, "Transient Stability Analysis of a Combined Cycle Power Plant Using Etap Software," *2017 IEEE 7th International Advance Computing Conference (IACC)*, Hyderabad, India, 2017, pp. 510–515. doi: 10.1109/IACC.2017.0111.
[39] J. Patel and M. Sinha, "Power System Transient Stability Analysis Using ETAP Software," *National Conference on Recent Trends in Engineering & Technology*, pp. 13-14, 2022.
[40] M. Al-jumaili, J. Rahebi, A. Akbas, and A. Farzamnia, "Economic dispatch optimization for thermal power plants in Iraq," *IEEE 2nd International Conference on Automatic Control and Intelligent Systems (I2CACIS)*, Kinabalu, 2017, pp. 140–143. doi: 10.1109/I2CACIS.2017.8239047.
[41] T. Hiyama and S. Koga, "Rule based economic dispatch for planning of thermal units operation," *IEEE Power Engineering Society Winter Meeting. Conference Proceedings (Cat. No.01CH37194)*, Columbus, OH, USA, 2001, vol. 3, pp. 1055–1060. doi: 10.1109/PESW.2001.917215.
[42] J. Zhu, "Optimization of Power System Operation," Hoboken, NJ, USA: John Wiley & Sons, Inc, 2015. doi: 10.1002/9781118887004.
[43] Po-Hung Chen and Hong-Chan Chang, "Large-scale economic dispatch by genetic algorithm," *IEEE Transactions on Power Systems*, vol. 10, no. 4, pp. 1919–1926, 1995, doi: 10.1109/59.476058.
[44] K. Mohamed-Nor and A. H. A. Rashid, "Efficient economic dispatch algorithm for thermal unit commitment," *IEEE Proceedings C Generation, Transmission and Distribution*, vol. 138, no. 3, p. 213, 1991, doi: 10.1049/ip-c.1991.0025.
[45] G. Huang and K. Song, "A simple two stage optimization algorithm for constrained power economic dispatch," *IEEE Transactions on Power Systems*, vol. 9, no. 4, pp. 1818–1824, 1994, doi: 10.1109/59.331436.
[46] Liu Shengsong, Hou Zhijian, and Wang Min, "A hybrid algorithm for optimal power flow using the chaos optimization and the linear interior point algorithm," *Proceedings. International Conference on Power System Technology*, Kunming, China, 2002, vol. 2, pp. 793–797. doi: 10.1109/ICPST.2002.1047508.
[47] X. Ding, "Interior point cutting plane method for optimal power flow," *IMA Journal of Management Mathematics*, vol. 15, no. 4, pp. 355–368, 2004, doi: 10.1093/imaman/15.4.355.
[48] G. L. Torres and V. H. Quintana, "Optimal power flow via interior point methods: an educational tool in Matlab," *Proceedings of 1996 Canadian Conference on Electrical and Computer Engineering*, Calgary, Alta, Canada, 1996, vol. 2, pp. 996–999. doi: 10.1109/CCECE.1996.548322.
[49] S. Granville, J. C. O. Mello, and A. C. G. Melo, "Application of interior point methods to power flow unsolvability," *IEEE Transactions on Power Systems*, vol. 11, no. 2, pp. 1096–1103, 1996, doi: 10.1109/59.496200.
[50] R. Ramos de Souza, A. Roberto Balbo, L. Nepomuceno, E. Cassia Baptista, E. Martins Soler, and R. Bento Nogueira Pinheiro, "A primal-dual interior/exterior point method, with combined directions and quadratic test in reactive optimal power flow problems," *IEEE Latin America Transactions*, vol. 15, no. 8, pp. 1413–1421, 2017, doi: 10.1109/TLA.2017.7994787.
[51] M. A. Rajpur, A. G. Memon, and K. Harijan, "Energy and Exergy Analysis of 210 MW Jamshoro Thermal Power Plant," *Mehran University Research Journal of Engineering and Technology*, vol. 35, no. 2, pp. 265–274, 2016.
[52] S. Klungtong and C. Chompoo-inwai, "Power flow monitoring and analysis for 24.6 MW at 6.9 kV bus Diesel Power Plant(DPP) using ETAP," *International Conference on Smart Grid and Clean Energy Technologies (ICSGCE)*, Chengdu, China, 2016, pp. 307–312. doi: 10.1109/ICSGCE.2016.7876074.
[53] Y. Rajashekar, P. Nandakumar, J. Philip, and A. Seshadri, "Techniques for practical qualitative approach using commercial power system simulation software for industrial applications," in *7th International Conference on Power Systems (ICPS)*, Pune, 2017, pp. 802–805. doi: 10.1109/ICPES.2017.8387399.
[54] H. Zhu, "The application of the ETAP Solftware in the Analysis and Simulation of Power Systems," *International conference energy and power engineering*, Hong Kong, 2014, vol. 1, pp. 209–213.
[55] R. A. Jabbar Khan, M. Junaid, and M. M. Asgher, "Analyses and monitoring of 132 kV grid using ETAP software," *International Conference on Electrical and Electronics Engineering - ELECO,* 2009, pp. 113–118, doi: 10.1109/ELECO.2009.5355219.
[56] N. Nisar, M. B. Khan, S. Gondal, and M. Naveed, "Analysis and optimization of 132KV grid using ETAP," *Power Generation System and Renewable Energy Technologies (PGSRET)*, Islamabad, 2015, pp. 1–6. doi: 10.1109/PGSRET.2015.7312188.

[57] C. J. Soni, P. R. Gandhi, and S. M. Takalkar, "Design and analysis of 11 KV distribution system using ETAP software," *International Conference on Computation of Power, Energy, Information and Communication (ICCPEIC)*, Melmaruvathur, Chennai, India, 2015, pp. 0451–0456. doi: 10.1109/ICCPEIC.2015.7259526.
[58] X. Qian, L. Wan, and H. Yang, "Transient Analysis for Electrical System of Power Plant Based on ETAP," *The Power Construction*, vol. 33, no. 3, pp. 74–78, 2012.
[59] A. H. Siddique, M. Hasan, S. Islam, and K. Rashid, "Prospective Smart Distribution Substation in Bangladesh: Modeling and Analysis," *Sustainability*, vol. 13, no. 19, p. 10904, 2021, doi: 10.3390/su131910904.

BIOGRAPHIES OF AUTHORS

Raheel Muzzammel received the B.Sc. degree in Electrical Engineering from the University of Engineering and Technology, Lahore, Pakistan in 2010 and the M.S. degree in Electrical Engineering from the University of Lahore, Lahore, Pakistan in 2013. He is currently working as an Assistant Professor at the University of Lahore, Lahore, Pakistan. His research interests include power system analysis, power system protection, artificial neural networks, power transmission lines, machine learning, microgrids, and smart grids. He can be contacted at email: raheelmuzzammel@gmail.com.

Rabia Arshad received the Master's degree in electrical engineering from the University of Lahore, Lahore in 2016 following her BSc. in Computer Engineering from the University of Engineering and Technology, Lahore. Currently, he is working as an Assistant Professor in the Department of Electrical Engineering in the University of Lahore, Lahore, Pakistan. She has an experience of more than 7 years in academia. Her research interests include communication systems and smart grids. She can be contacted at email: rabia.arshad@ee.uol.edu.pk.